Water **2015**, *7*, 5849-5875; doi:10.3390/w7105849

OPEN ACCESS

water

ISSN 2073-4441
www.mdpi.com/journal/water

Article

Water Discharge and Sediment Load Changes in China: Change Patterns, Causes, and Implications

Chong Jiang [1,2,3,4,*], Linbo Zhang [1,4], Daiqing Li [1,4] and Fen Li [1,4,*]

[1] State Key Laboratory of Environmental Criteria and Risk Assessment, Chinese Research Academy of Environmental Sciences, Beijing 100012, China; E-Mails: zhanglb@craes.org.cn (L.Z.); lidq@craes.org.cn (D.L.)
[2] College of Global Change and Earth System Science, Beijing Normal University, Beijing 100875, China
[3] Joint Center for Global Change Studies, Beijing 100875, China
[4] Key Laboratory of Regional Eco-Process and Function Assessment and State Environment Protection, Chinese Academy of Environmental Sciences, Beijing 100012, China

* Authors to whom correspondence should be addressed; E-Mails: jiangchong1987@gmail.com (C.J.); lifen@craes.org.cn (F.L.); Tel./Fax: +86-010-84915171 (C.J. & F.L.).

Academic Editor: Yingkui Li

Received: 6 August 2015 / Accepted: 8 October 2015 / Published: 26 October 2015

Abstract: In this research, monthly hydrological and daily meteorological data were collected across China for the period 1956–2012. Modified Mann–Kendall tests, double mass curve analysis, and correlation statistics were performed to identify the long-term trends and interrelation of the hydrometeorological variables and to examine the influencing factors of streamflow and sediment. The results are as follows: (1) In the last 60 years, the streamflow in northern China has shown different decreasing trends. For the southern rivers, the streamflow presented severe fluctuations, but the declining trend was insignificant. For the streamflow in western China, an increasing trend was shown. (2) In the northern rivers, the streamflow was jointly controlled by the East Asian monsoon and westerlies. In the southern rivers, the runoff was mainly influenced by the Tibet–Qinghai monsoon, the South Asian monsoon, and westerlies. (3) Sediment loads in the LCRB (Lancang River Basin) and YZRB (Yarlung Zangbo River Basin) did not present significant change trends, although other rivers showed different degrees of gradual reduction, particularly in the 2000s. (4) Underlying surface and precipitation changes jointly influenced the streamflow in eastern rivers. The water consumption for industrial and residential purposes, soil and water

conservation engineering, hydraulic engineering, and underlying surface changes induced by other factors were the main causes of streamflow and sediment reduction.

Keywords: streamflow; sediment load; precipitation; monsoon; soil and water conservation engineering

1. Introduction

Global warming caused by human-induced emissions of greenhouse gases is accelerating the global hydrological cycle [1]. The accelerated hydrological cycle is in turn altering the spatial-temporal patterns of precipitation, resulting in increased occurrences of precipitation extremes that cause increased occurrences of floods and droughts in many regions of the world [2], including China [3–5]. As a vital natural resource, water is fundamental for the sustainable development of the economy, ecosystem, and biodiversity. Therefore, water security and related implications for ecosystem and river diversity, particularly the variability and availability of regional water resources under the influences of climatic change and human activities, have been discussed in recent years [6–8]. Much attention has been given to water resource changes and their effects on the economic society by the international community. For example, the Intergovernmental Panel on Climate Change (IPCC) has reviewed changes in the global hydrological cycle and has assessed the impacts of climatic change on water resources [9]. Many countries, such as the United Kingdom, have addressed the impact of climatic change on water resource variation [10]. The climatic changes of China are controlled mainly by winter and summer monsoons [11]. Generally, precipitation in southwest China is greater than that in northwest China; these patterns are controlled mainly by the monsoon system and the effects of topography [12]. Rainy seasons in eastern China hinge on progress and retreat of the East Asian monsoon. Detailed information on the evolution of summer Asian monsoons and the associated propagation of rain belts has been reported by Ding [13].

River sediment is an important aspect of land surface processes and global change research. River sediment generation, transportation, and river delta response have become important aspects of Earth system science. In 1968, Holeman [14] investigated global sediment discharge by using global hydrological data; further research was conducted by Holland [15]. Walling and Fang [16] investigated the temporal variation of 145 rivers by using long-term data (longer than 25 years) in Asia, Europe, and North America. They reported that the sediment discharge in more than 50% of analyzed rivers presented upward or downward trends, the latter of which was dominant. However, in the remaining 50%, the sediment flux essentially remained stable [17]. A study of the sediment load in Russia showed that of the 20 rivers flowing into the Arctic Ocean, 35% showed increasing trends, 60% presented declining trends; only 5% remained stable [18]. Similar research was conducted by Liu [19], Subramainian [20], and Siakeu [21] for major rivers of Asia, India, and Japan, respectively. This research revealed that human activities, particularly reservoir and dam construction, were the main causes of sediment flux reduction.

Many researchers investigated the sediment and streamflow change in major rivers of China. The Yangtze River Basin (YARB) [22], Yellow River Basin (YRB) [23], Huai River Basin (HURB) [24], Liao River Basin (LRB) [25], and Songhua River Basin (SRB) [26] showed different degrees of

decreasing trends. However, the sediment flux in western rivers such as the Yarlung Zangbo River Basin (YZRB) and Lancang River Basin (LCRB) remained stable or increased slightly. The Yellow and Yangtze rivers are two of the largest rivers in China and therefore receive more attention. Yang [27] considered that reservoir and dam construction was the main reason of sediment reduction in the Yangtze River. Miao [23] reported that reservoir construction, reduced precipitation, soil and water conservation projects jointly induced sediment reduction in the Yellow River. So far, the focus in China has been mostly on regional water and sediment resources. On the basis of instrument records of streamflow and sediment, many scholars conducted research in different river basins in China to reveal different changing patterns of runoff and sediment. Most of these studies are based on the monitoring data of individual rivers without considering the impacts of water and sand resource consumption of the economic society within the river basin. Regarding spatial scale, most studies completed thus far are based on one river basin; few are based on a national scale. An acceptable evaluation of water and sediment resources requires sufficient hydrometeorological data and extensive data-driven analysis, which is the motivation for the current study. Further, possible causes of precipitation and streamflow and sediment resource variation need to be investigated, and the related implications should be discussed.

Therefore, the objectives of this study are to (1) investigate streamflow and sediment changes in major rivers in China; (2) determine the streamflow changes and their relationship with precipitation, monsoons, and water consumption for industrial and residential purposes; (3) determine regional sediment load changes and their relationship with hydraulic engineering, soil and water conservation engineering, and underlying surface changes induced by human activities; and (4) discuss the relationship between sediment and runoff changes and their relationship with specific events, the implications of which will also be discussed. The primary goal of this study is to evaluate the impact of climate change and human activities on streamflow and sediment load and to provide basic information for water and soil resources management in this region.

2. Data and Methodology

2.1. Data Collection and Processing

In this study, annual precipitation data from 725 rain gauge stations for the period 1951–2012 were obtained from the National Climate Center (NCC) of the China Meteorological Administration (CMA). The quality of meteorological data was firmly controlled [28]. To guarantee the accuracy of the results, the data was preprocessed as follow before the analysis. The observational data of missing data years of more than 5 years (including 5 years) were excluded. The time series data of partial relocation stations were unified, and the remaining missing observation data were completed with a linear regression method and adjacent station interpolation to ensure the integrity of the time series. The missing data in 725 stations only accounted for less than 5% of total data amount. The regional averages refer to the arithmetic mean value of the stations within a region. Annual precipitation average was, thus, calculated from these records using the Thiessen Polygon method for each river basin.

The consecutive monthly data of streamflow and sediment yields from the 30 gauge stations were collected for the same period from Ministry of Water Resources (MWR). The hydrologic data from the 30 gauge stations listed in Table 1 were used to analyze changes in streamflow and sediment load.

Figure 1 and Table 1 provide information on the station location and associated drainage area. It is worth to address is that, the Xinjiang Inland River Basin and the Hexi Inland River Basin (HIRB) in northwestern China are composed of many tributaries. Therefore, to reflect the overall change in streamflow, we summed the streamflow in tributary data to represent the runoff of the entire basin. In southwestern China, although many large rivers are present, we selected as study objects only two river systems, the LCRB and YZRB, considering data availability.

The daily discharge was computed from the water level by using previously calibrated discharge-water level curves. Water was sampled at fixed intervals, and suspended sediment concentration was obtained by measuring water samples in the laboratory. All the measurements of water level, discharge, SSC followed national standards issued by the Ministry of Water Conservancy, and were printed in the China Gazette of River Sedimentation [29]. Sediment loads refers to the suspended fraction only, whereas bedload was excluded due to its difficulty in field sampling. Measurement of the sediment loads was on the basis of standard procedures [30,31]. Errors in calculating sediment load were introduced through the low frequency of sampling, rather than continuous monitoring, which is likely to underestimate sediment load during peak hours. The monthly and annual streamflow and sediment load at the gauging stations were derived from the daily measured data. The accuracy and consistency of all the data used in this study have been checked out by the corresponding agencies before their release. In instances when discharge data were missing, we used discharge data from similar rainfall conditions at other times as a replacement, and the missing data in 30 stations only accounted for less than 3% of total data amount.

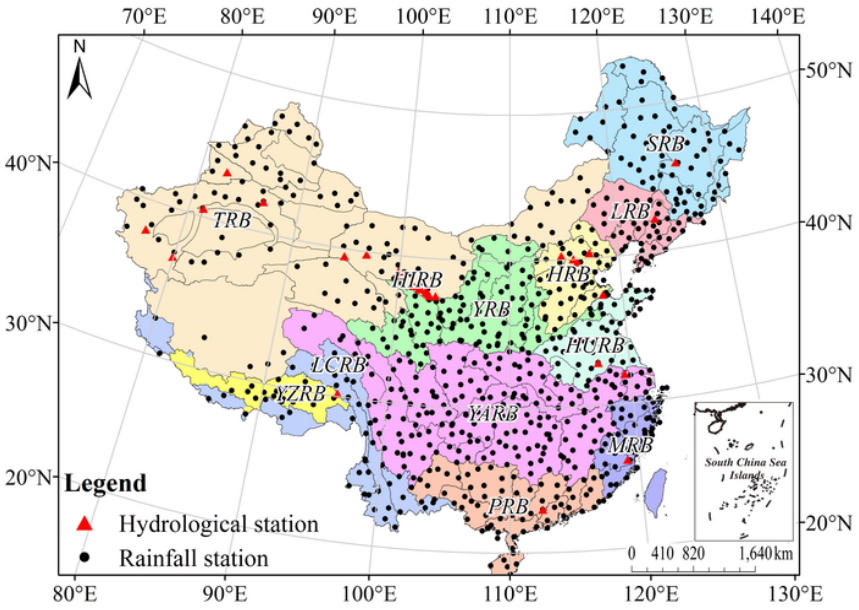

Figure 1. Distribution of 12 major basins in China showing gauge stations (red triangles) and meteorological stations (black dots) used in this study.

1:100,000-scale land use maps in 1985 and 2010 were respectively obtained from the Earth System Science Data Sharing Platform and The Remote Sensing Monitoring and Assessment of Decadal Changes of National Eco-environment (2000–2010) project group. The digital elevation model (DEM),

the Monitoring Report of Soil and Water Loss in China, and other maps were obtained from the Earth System Science Data Sharing Platform.

Table 1. Summary of gauging stations and hydrological characteristics in the 12 major basins in China. DA is the drainage area.

ID	Gauge Station	Basin (Abbreviation)	Location	Longitude (N°)	Latitude (E°)	DA (km^2)	Time Span
1	Lijin	Yellow River Basin (YRB)	Mainstream	118°15′	37°29′	752,032	1952–2012
2	Datong	Yangtze River Basin (YARB)	Mainstream	117°03′	32°37′	1,705,383	1950–2012
3	Wujiadu	Huai River Basin (HURB)	Mainstream	117°23′	32°54′	121,330	1950–2011
4	Zhangjiafen	Hai River Basin (HRB)	Bai River	116°10′	39°48′	8506	1954–2011
5	Xiahui		Chao River	117°18′	40°22′	5340	1961–2011
6	Shixiali		Sanggan River	114°43′	40°16′	23,944	1952–2011
7	Xiangshuipu		Yang River	109°40′	38°01′	14,507	1952–2011
8	Yanling		Yongding River	115°49′	40°01′	43,674	1952–2011
9	Haerbin	Songhua River Basin (SRB)	Mainstream	126°32′	45°48′	389,769	1955–2012
10	Tieling	Liao River Basin (LRB)	Mainstream	123°43′	42°13′	120,764	1954–2012
11	Gaoyao	Pearl River Basin (PRB)	Xi River	112°27′	23°01′	351,535	1957–2011
12	Zhuqi	Southeast Rivers Basin (Min River Basin, MRB)	Mainstream	119°06′	26°08′	54,500	1950–2011
13	Nuxia	Southwestern Rivers Basin (Yarlung Zangbo River, YZRB)	Mainstream	95°05′	31°17′	191,235	1956–2009
14	Xiangda	Southwestern Rivers Basin (Lancang River Basin, LCRB)	Mainstream	96°28′	32°12′	17,909	1956–2012
15	Dajingxia Reservoir	Hexi Inland River Basin (HIRB)	Dajing River	103°24′	37°28′		1961–2010
16	Gulang		Gulang River	102°52′	37°27′		1961–2010
17	Huangyanghe Reservoir		Huangyang River	102°44′	37°35′		1961–2010
18	Zamusi		Zamu River	102°34′	37°42′		1961–2010
19	Nanying Reservoir		Jinta River	102°31′	37°48′	68,300	1961–2010
20	Jiutiaoling		Xiying River	102°03′	37°52′		1961–2010
21	Shagousi		Dongda River	101°55′	37°58′		1961–2010
22	Xidahe Reservoir		Xida River	101°23′	38°03′		1961–2010
23	Changmapu		Shule River	96°51′	39°49′		1961–2010

Table 1. *Cont.*

ID	Gauge Station	Basin (Abbreviation)	Location	Longitude (N°)	Latitude (E°)	DA (km^2)	Time Span
24	Dangchengwan	Hexi Inland River Basin (HIRB)	Dang River	94°53′	39°30′		1961–2010
25	Yingluoxia		Hei River	99°55′	38°57′	68,300	1961–2010
26	Binggou		Beida River	101°56′	37°54′		1961–2010
27	Kaqun	Xinjiang Inland River Basin (Tarim River Basin, TRB)	Yeerqiang River	76°54′	37°59′	50,248	1957–2011
28	Tongguziluoke		Yulongkashi River	79°55′	36°49′	14,575	1957–2011
29	Yanqi		Kaidu River	86°34′	42°02′	22,516	1957–2011
30	Alaer		Mainstream	81°19′	40°32′	127,900	1957–2011

2.2. Methodology

2.2.1. Mann–Kendall Test for Monotonic Trend

To analyze the long-term trends of hydrometeorological variables, the non-parametric Mann–Kendall test [32,33] was applied. This method has been widely used to detect trends in climate and streamflow time series [34]. In the Mann–Kendall test, the null hypothesis H_0 states that $x_1,..., x_n$ are samples of n independent and identically distributed random variables with no seasonal change. The alternative hypothesis H_1 for a two-sided test defines the distributions of x_k and x_j as non-identical for all $k, j \leq n$; with $k \neq j$. The test statistic S is given as

$$S = \sum_{i=1}^{n-1} \sum_{k=i+1}^{n} \operatorname{sgn}\left(x_k - x_i\right) \tag{1}$$

$$\operatorname{sgn} = \begin{cases} +1 & \theta > 0 \\ 0 \quad if & \theta = 0 \\ -1 & \theta < 0 \end{cases} \tag{2}$$

If the dataset is independent and identically distributed, the mean of S will be zero, and the variance of S will be:

$$\operatorname{var}(S) = \left[n(n-1)(2n+5) - \sum_{j=1}^{m} t_j \left(t_j - 1\right)\left(2t_j + 5\right) \right] \Big/ 18 \tag{3}$$

where n is the number of data points, t is the extent of a given time, m is the number of tied groups, and t_j is the number of data points in the j-th group. A tied group is a set of data points having the same value. A normalized test statistic Z can be computed on the basis of S as:

$$Z = \begin{cases} \dfrac{S-1}{\sqrt{\operatorname{var}(S)}} & S > 0 \\ 0 & S = 0 \\ \dfrac{S+1}{\sqrt{\operatorname{var}(S)}} & S < 0 \end{cases} \tag{4}$$

When the significance levels are set at 0.01, 0.05, and 0.1, $|Z_\alpha|$ is 2.58, 1.96, and 1.65, respectively. At a certain significance level, if $|Z| > |Z_\alpha|$, the null hypothesis H_0 is rejected. That is, the trend is significant at the set level of significance. Otherwise, no significant trend exists.

In the Mann–Kendall test, the slope estimated by using the Theil–Sen estimator [35,36] is usually considered to detect the monotonic trend and to indicate the variable quantity in the unit time. It is a robust estimate of the magnitude of a trend and has been widely used to identify the slope of a trend line in a hydrological or climatic time series [37]. The estimator is given as:

$$\beta = Median\left(\frac{x_j - x_l}{j - l}\right) \forall 1 < l < j \tag{5}$$

where $1 < l < j < n$, β is the median overall combination of record pairs for the entire dataset and is resistant to extreme observations. A positive β denotes an increasing trend, and a negative β indicates a decreasing trend.

2.2.2. Modified Mann–Kendall Test (Mann–Kendall Test with Trend-Free Pre-whitening)

The Mann–Kendall test assumes that the series is independent and the series is not robust against autocorrelation. However, certain hydrological time series may frequently display statistically significant serial correlation. This may lead to a disproportionate rejection of the null hypothesis of no trend, whereas the null hypothesis is actually true. Therefore, the effect of serial correlation is a major source of uncertainty in testing and interpretation trends. To eliminate the influence of serial correlation, "pre-whitening" was proposed by Von Storch [38] to remove the lag one serial correlation (r_1) from the time series. This method has been applied in an increasing number of studies [23,26,39].

To determine whether the observed dataset is serially correlated, the significance of the lag-1 serial correlation (r_1) should be tested at the 0.10 significance level. r_1 is calculated by using the following Equation [23,26]:

$$r_k = \frac{\frac{1}{n-k}\sum_{i=1}^{n-k}\left(x_i - \bar{x}\right)\left(x_{i+k} - \bar{x}\right)}{\frac{1}{n}\sum_{i=1}^{n}\left(x_i - \bar{x}\right)^2} \tag{6}$$

If $\frac{-1-1.645\sqrt{n-2}}{n-1} \le r_1 \le \frac{-1+1.645\sqrt{n-2}}{n-1}$, the time series is assumed to be independent at the 0.10 significance level and can be subjected to the original Mann–Kendall test. Otherwise, the effect of serial correlation should be removed from the time series by pre-whitening prior to application of the Mann–Kendall test. The Mann–Kendall test is then used to detect trends in the residual series. The new time series is obtained as [40].

$$x_i^{'} = x_i - (\beta \times i) \tag{7}$$

The r_1 value of this new time dataset is calculated and used to determine the residual series as:

$$y_i^{'} = x_i^{'} - r_1 \times -x_{i-1}^{'} \tag{8}$$

The value of $\beta \times i$ is added again to the residual dataset as:

$$y_i = y_i^{'} + (\beta \times i) \tag{9}$$

The y_i series is then subjected to trend analysis.

2.2.3. Double Mass Curve

Double mass curve analysis is a simple and practical visual method widely used in the study of the consistency and long-term trend test of hydrometeorological data [41]. This method was first used to analyze the consistency of precipitation data in Susquehanna watershed, Pennsylvania, USA [42]; a theoretical explanation was later reported [43]. The theory of the double mass curve is based on the fact that a plot of two cumulative quantities during the same period exhibits a straight line if the proportionality between the two remains unchanged; the slope of the line represents the proportionality. This method can smooth a time series and suppress random elements in the series; thus, it can show the main trends of the time series. In the last 30 years, Chinese scholars analyzed the effects of soil and water conservation measures and land use/cover changes on streamflow and sediment by using this method and have achieved good results [44]. In the present study, double mass curves of sediment *versus* streamflow were plotted for the different periods to detect the relationship change before and after transition years. The appearance of the inflection point denotes that the relationship between the sediment and streamflow begins to change significantly [44].

3. Variation of Streamflow and Sediment Load

3.1. Overall Change of Streamflow

In this study, we defined the northern rivers and southern rivers as those north and south of the eastern monsoon zone in China, respectively. Therefore, the northern rivers include the YRB, HRB, LRB, SRB, and HURB; the southern rivers include the Pearl River Basin (PRB), YARB, and Min River Basin (MRB); and the western rivers include the Tarim River Basin (TRB), HIRB, LCRB, and YZRB. Based upon the years of average runoff (Table 2), the order of runoff in the southern rivers was YARB (8944.8×10^8 m^3) > PRB (2166.4×10^8 m^3) > MRB (532.7×10^8 m^3); that in the northern rivers was SRB (404.7×10^8 m^3) > YRB (299.2×10^8 m^3) > HURB (266.9×10^8 m^3/a) > LRB (29.3×10^8 m^3) > HRB (18.1×10^8 m^3); and that in the western rivers was YZRB (312.5×10^8 m^3) > LCRB (247.3×10^8 m^3) > TRB (157.3×10^8 m^3) > HIRB (44.0×10^8 m^3). It should be noted that Xiangda Station, which represents the LCRB, is located at the source area of LCRB; therefore, the streamflow was smaller than that in the entire basin. Actually, the average streamflow in the downstream region of the LCRB was 740.5×10^8 m^3 [45].

Figure 2a,b show the cumulative curve of the streamflow in the major rivers. The cumulative curves of YARB, PRB, MRB, LCRB, YZRB, TRB, and HIRB, presented linear increasing trends with essentially no fluctuation or inflection point. Among them, the runoff in the HIRB showed a significant increasing trend at 0.16×10^8 m^3/a, $P < 0.001$. That of other basins fluctuated near the mean level, as shown in Figure 3; the interdecadal anomalies are shown in Table 3. For the northern rivers, the cumulative curve of streamflow in HURB presented complicated changes. The overall direction was a straight line, indicating severe fluctuation on the interannual scale, and no obvious trend was found. The other northern rivers generally presented convex curves or lines, indicating that runoff in these rivers showed decreasing trends (Figure 3). As shown in Table 4, the order of decrease rate was YRB (-7.25×10^8 m^3/a, $P < 0.001$) > SRB (-3.32×10^8 m^3/a, $P < 0.001$) > HRB (-0.69×10^8 m^3/a, $P < 0.001$) > LRB (-0.48×10^8 m^3/a, $P < 0.001$).

Table 2. Average annual streamflow and sediment load.

Basins	Water Discharge (10^8 m^3)	Sediment Load (10^4 t)
HRB	18.1	795.1
HURB	266.9	881.4
YRB	299.2	76,655
LRB	29.3	1112.9
SRB	404.7	598.8
MRB	532.7	573.3
PRB	2166.4	6274.6
YARB	8944.8	40791
HIRB	44.0	–
TRB	157.3	–
YZRB	312.5	1710.4
LCRB	247.3	341.0

3.2. Overall Change in Sediment Load

Figure 2c,d show the cumulative curve of the sediment load in the major rivers. No obvious convex state was presented in those of LCRB and YZRB, which means the sediment discharge variation had no significant trend. The cumulative curve of sediment load in other rivers showed obvious convex shapes, which denote that the sediment had different degrees of gradual reduction. In particular, after 2000, the decrease was between 59.1% and 98.7% (Table 3). In the southern rivers, the decrease in the 2000s was between 59.1% and 63.4%, with YARB showing the largest value. In the northern rivers, the decrease was between 59.4% and 98.7%; LRB and HRB were reduced by 97.6% and 98.7%, respectively (Table 3).

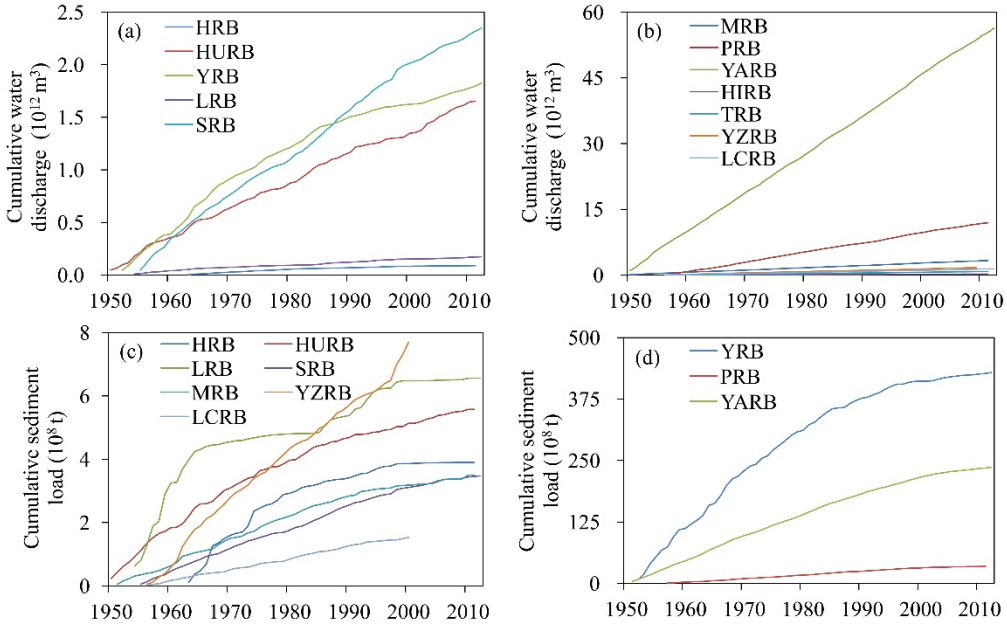

Figure 2. Cumulative curves of (**a**), (**b**) water discharge and (**c**), (**d**) sediment discharge in major basins in China, during 1950–2012.

Table 3. Interdecadal anomalies of water discharge and sediment load. The reference value is the average value during the 1950s to 1960s.

Basins	Change in Water Discharge (%)				Change in Sediment Load (%)			
	1970s	1980s	1990s	2000s	1970s	1980s	1990s	2000s
HRB	–18.6	–55.9	–56.4	–84.6	–35.0	–77.5	–77.2	–98.7
HURB	–27.8	0.1	–45.5	–6.5	–43.4	–46.8	–73.7	–69.6
YRB	–36.4	–41.5	–71.2	–67.5	–26.0	–47.3	–67.8	–88.7
LRB	–56.9	–36.8	–27.3	–62.8	–90.2	–80.3	–59.9	–97.6
SRB	–31.6	–2.9	–4.6	–43.4	–21.3	7.7	–19.6	–59.4
MRB	–1.7	–2.6	4.2	–5.4	–1.6	–13.4	–49.0	–63.4
PRB	11.2	–4.0	13.3	–6.4	10.9	14.7	4.4	–59.1
YARB	–6.1	–0.9	5.8	–5.7	–13.0	–10.9	–29.7	–63.1
YZRB	–6.6	–14.2	–4.5	5.2	–14.9	–24.0	–5.2	–
LCRB	–1.4	19.3	1.7	14.1	5.7	39.4	–14.4	–

Table 4. Results of Sen's slope estimator and the Z value by using linear regression and the Mann–Kendall test, respectively.

Basins	Water Discharge (10^8 m^3)			Sediment Load (10^4 t)		
	Slope	Z	Significance	Slope	Z	Significance
HRB	−0.69	−6.96 **	$P < 0.001$	−46.96	−6.73 **	$P < 0.001$
HURB	−1.50	−1.49	$P > 0.1$	−25.35	−5.42 **	$P < 0.001$
YRB	−7.25	−6.01 **	$P < 0.001$	−2300	−6.58 **	$P < 0.001$
LRB	−0.48	−3.2 *	$P < 0.01$	−55.33	−4.90 **	$P < 0.001$
SRB	−3.32	−3.37 **	$P < 0.001$	−8.44	−4.11 **	$P < 0.001$
MRB	−0.53	−0.58	$P > 0.1$	−9.74	−4.10 **	$P < 0.001$
PRB	−2.04	−0.98	$P > 0.1$	−77.49	−3.31 **	$P < 0.001$
YARB	−5.72	−0.36	$P > 0.1$	−6000	−6.73 **	$P < 0.001$
HIRB	0.16	2.81 *	$P < 0.01$	–	–	–
TRB	0.10	0.80	$P > 0.1$	–	–	–
YZRB	0.20	0.40	$P > 0.1$	6.12	0.47	$P > 0.1$
LCRB	0.61	1.58	$P > 0.1$	−0.96	−0.67	$P > 0.1$

Note: "*" and "**" mean the correlation coefficient reach the significance level of 0.01 and 0.001, respectively.

3.3. Pattern of Changes in Streamflow and Sediment Load

Figures 3 and 4 show respectively the temporal variation and double mass curves of sediment load and streamflow in the 12 major rivers in China. On the whole, the variation of streamflow *versus* sediment can be divided into three categories. In the first, the streamflow was stably maintained, but the sediment load was reduced (HURB, YARB, MRB, PRB). In the second, the streamflow and sediment load were both reduced (YRB, LRB, HRB, SRB). In the third, both water and sediment discharge remained stable (LCRB, YZRB).

3.3.1. Streamflow Remained Stable and Sediment Load Reduced

In the HURB, the streamflow and sediment discharge experienced continuous declines before 1978 (Figures 3a and 4a). Since the early 1980s, and particularly in the 1990s, an obvious decrease in sediment discharge occurred. This result was due mainly to the effects of soil and water conservation projects in the HURB with areas of 1.53 × 10^4 km^2 and 1.04 × 10^4 km^2 in the 1980s and 1990s, respectively. Shi [24] reported that the soil erosion amount of the small watershed in the upper reaches of the Huai River was reduced 77%–85% after implementation of engineering projects.

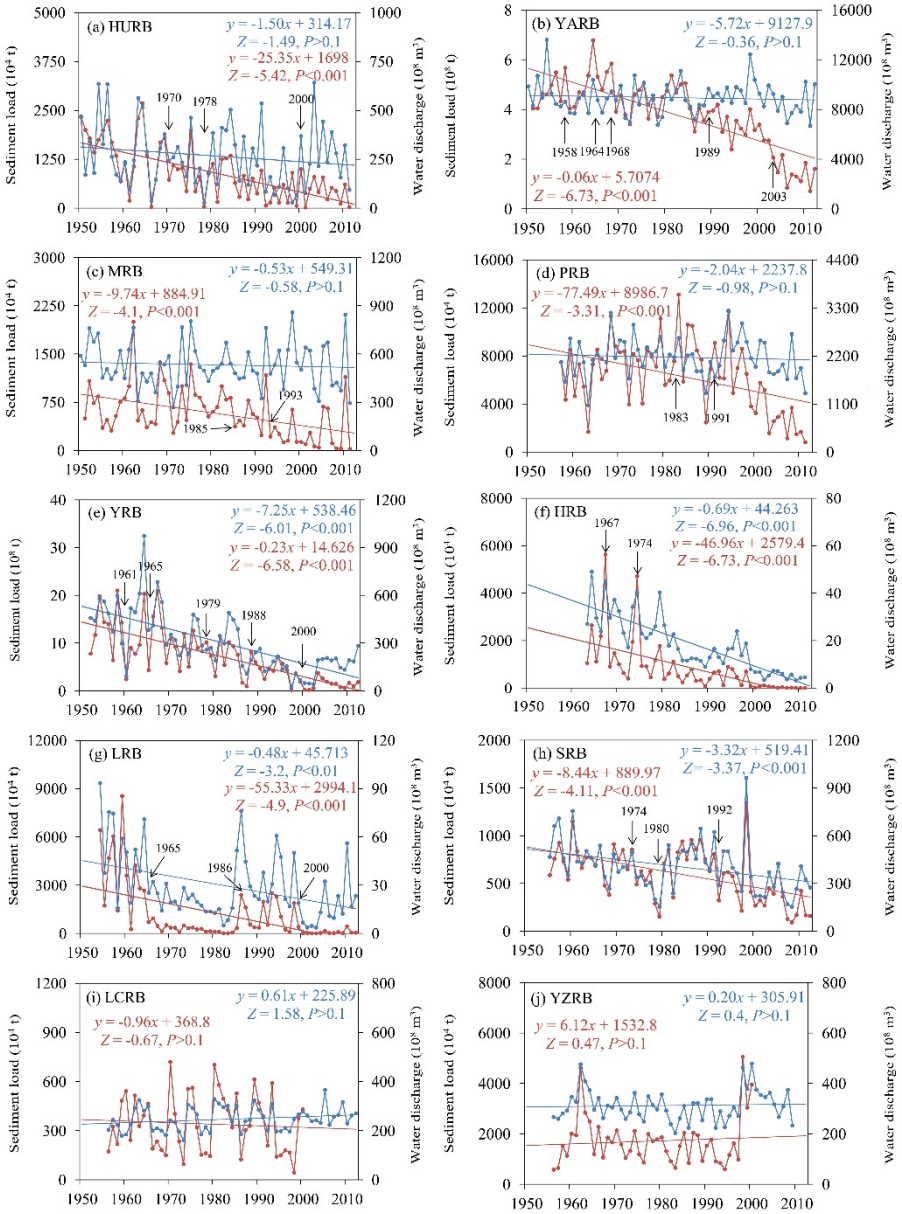

Figure 3. Interannual variability of streamflow and sediment load in major basins in China during 1950–2012. Blue and red lines represent changes in water discharge and sediment discharge, respectively.

In the YARB, the streamflow variation was relatively stable; however, the sediment load decreased significantly (Figures 3b and 4b). The sediment yields in 1956, 1958, and 1963–1968 were obviously

high, which is likely attributed to large-scal edeforestation activities such as "Devastating Forests for Arable Land". After 1969, the sediment load value suddenly dropped. This result is likely attributed to the Danjiangkou Reservoir operation that began in 1968, which intercepted a large amount of sediment. After 1989, the sediment yield decreased again, which could have been caused by three aspects. Firstly, a series of ecological engineering projects was conducted since 1982, particularly the Changzhi Project launched in 1989. Secondly, the reservoirs were constructed in the mainstream and tributaries of the Yangtze River. Thirdly, the amount of sand dredging increased annually. The total amount in 1990–2002 was 5×10^7 t. After 2003, the sediment load decreased again, which was mainly caused by operation of the Sanxia Reservoir in 2003. In 2012, sedimentation in Sanxia Reservoir reached 14.37×10^8 t.

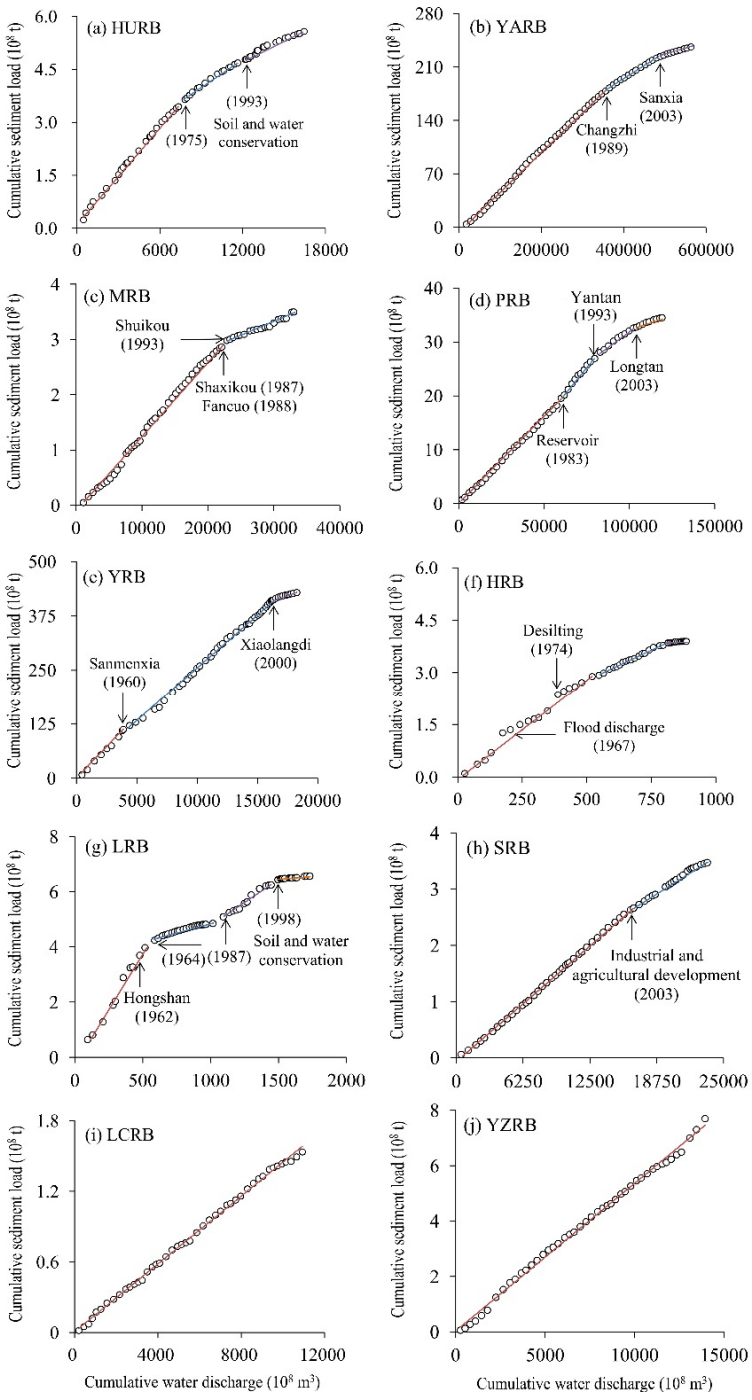

Figure 4. Double mass curve of streamflow *versus* sediment load.

For MRB, as observed by Zhuqi Station, sediment load changed with streamflow variation before 1985, although the amplitude of the sediment was larger than that of the streamflow (Figures 3c and 4c). After 1985 and 1993, we detected two distinct decreasing processes obviously related to reservoir construction such as the Shaxikou hydropower station in 1987, Fancuo Dam in 1988, and the Shuikou hydropower station in 1993. In particular, the sedimentation of Shuikou Dam accounted for 86% of the total amount of sediment in the MRB. An additional factor is that the annual sand dredging amount in Mawei near Shuikou Dam was 1×10^7 t after the late 1980s. The streamflow in Gaoyao Station of PRB was stable, although the sediment load decreased significantly (Figures 3d and 4d). Before 1983, the sediment load fluctuated with streamflow change and maintained a consistent pace. In 1983–1991, the sediment load increased obviously, which may related to the construction of multiple reservoirs. Since 1994, the sediment load presented a sharp decline, which is mainly attributed to the sediment-retaining functions of reservoirs and dams such as Yantan Reservoir in the Hongshui River (operated in 1993) and Longtan Reservoir (operated in 2003).

3.3.2. Streamflow and Sediment Load Reduced Together

In the YRB, HRB, LRB, and SRB, the water and sediment discharge showed clear downward trends. In YRB, as observed by Linjin Station, the sediment loads in 1961–1965, 1980–1988, and 2000–2012 were lower than the mean level (Figures 3e and 4e). The low point in 1961 reflected the operation of Sanmenxia Reservoir, which began to retain water and sediment. In 1965, the operation mode of this reservoir changed to begin storing clear water and releasing muddy sediment; therefore, the sediment load recovered slightly. After 1980, the sediment load reduced again, with the following possible causes: Firstly, the water diversion project began operation, which reduced the streamflow and sediment discharge. Secondly, the soil and water conservation projects in the upstream function are functioning efficiently; thus, the water discharge is reduced in the lower reaches. Thirdly, the rainfall is concentrated mainly in the midstream region with less soil loss area; thus, the sediment is reduced downstream. In the early 2000s, the sediment and streamflow reduced again, mainly due to the water diversion projects and water reservoirs operating in the upstream region, such as Xiaolangdi Reservoir in 1999.

In the HRB, the sediment and streamflow after the 1980s was maintained at relatively low levels, the sediment load approached zero since 2000 (Figures 3f and 4f). The abnormally high sediment load in 1967 and 1974 was due to the desilting effect of Guanting Reservoir during the flood season through high rainfall and runoff. In the LRB, the sediment and water discharge presented periodic changes (Figures 3g and 4g). Before the 1960s, strong rainfall caused severe soil erosion, thereby inducing sediment load increases. After 1964, the sediment load decreased significantly due to the operation of Hongshan Reservoir in 1962. Until 1999, the sedimentation in Hongshan Reservoir reached 9.41×10^8 m^3, accounting for 58% of the total storage capacity. Severe fluctuation of sediment and streamflow occurred in 1985–2000, which was caused mainly by rainfall.

In the SRB, the streamflow and sediment discharge decreased at the same pace (Figures 3h and 4h). On the interdecadal scale, the streamflow and sediment discharge experienced "low-high-low" alternating variation processes in the 1970s to 1990s, which were mainly affected by precipitation. In addition, agricultural and industrial development since the beginning of the 1960s also accelerated the water consumption for industrial and residential purposes. Although some large- and medium-sized

reservoirs are located in the upstream regions of Songhua River, the reciprocal relationship between runoff and sediment has been relatively good, and no obvious anomalies have been detected. This result occurred essentially because the vegetation coverage in the source area is relatively high, and density of population is low; thus, the river is seldom disturbed by human activities.

3.3.3. Both Streamflow and Sediment Discharge Remained Stable

Both streamflow and sediment discharge in the LCRB and YZRB maintained stability. No significant upward or downward trends were detected, and fluctuations of streamflow *versus* sediment have been essentially consistent (Figures 3i,j and 4i,j). Actually, the vegetation coverage is good, the population density in the YZRB and LCRB is relatively low, and the level of economic development and social construction is also relatively low. Thus; the streamflow and sediment are seldom affected by human activities, and presented a good correlation among rainfall, streamflow, and sediment.

4. Influencing Factors of Streamflow Variation

4.1. Precipitation

In general, climate change is mainly characterized by temperature and precipitation variability. Precipitation drives runoff and hence directly influences the discharge of a river. Figure 5 shows precipitation changes in the major rivers and in the entire country that occurred during the past 60 years. China's precipitation experienced a "decrease, increase, decrease, increase, decrease" pattern. The 1950s was a rainy decade; the average rainfall reached 820.3 mm, which was the highest value recorded in several decades. After 1960, precipitation began to decrease. Levels were low in the 1980s and increased slightly in the 1990s. After 2000, the overall trend obviously reduced. The SRB and LRB experienced a rainy period in the 1950s that decreased in the 1960s and 1970s. The 1980s and 1990s presented slight increases that decreased again in the 2000s. Precipitation in the YRB essentially showed a decreasing trend by decade with lowest values occurring in the 1990s. After 2000, however, the level increased slightly. Rainfall in the TRB and HIRB increased by decade; however, the YZRB and LCRB presented decreasing trends since the 1960s. For the southern rivers including YARB, MRB, and PRB, changes in precipitation were consistent. Levels were lowest in the 1950s, increased in the 1960s and 1970s, and fell slightly in the 1980s before returning to the less-rainfall stage in 2000.

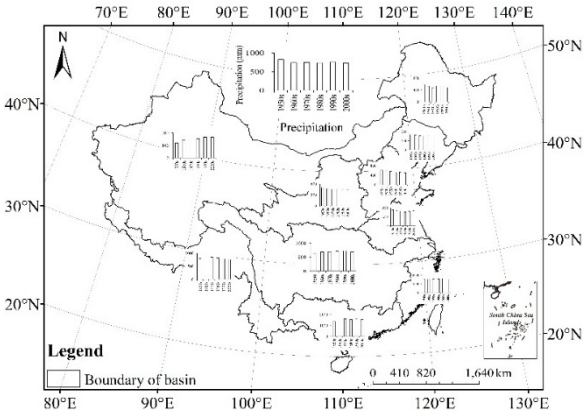

Figure 5. Interdecadal rainfall changes in the main basins in China during the 1950–2012.

Since the Reform and Opening-up policy was implemented in 1979, the demand for water resources increased substantially, and the streamflow in some rivers showed different degrees of decreasing trend (Figure 3). Therefore, we divided the streamflow sequence into two periods of before and after 1980 to explore the relationship between streamflow and precipitation (Figure 6). The subsection fitting lines of precipitation *versus* runoff represent the runoff depth produced by rainfall in 1950–1979 and 1980–2010, respectively. Assuming that the precipitation had no significant change on the basin scale, changes in the relationship of precipitation and streamflow can reflect the influence of the underlying surface on the original hydrological process. In the northern rivers, the fitting lines of rainfall-runoff in the HRB (Figure 6a), YRB (Figure 6c), and SRB (Figure 6e) moved downward during 1980–2010 comparing with that occurring in 1950–1979.

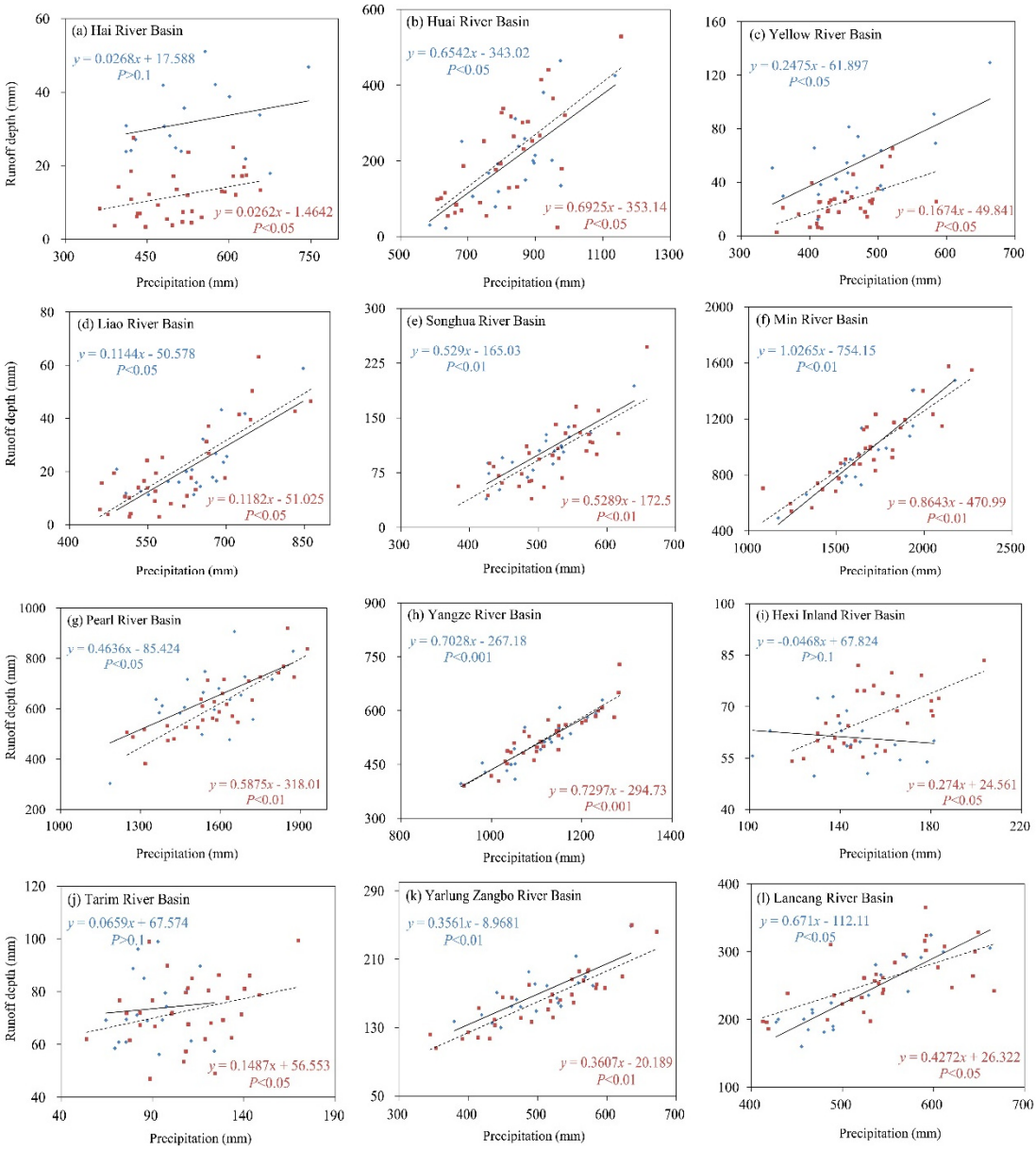

Figure 6. Subsection fitting lines of precipitation *versus* streamflow in 1950–1979 *versus* those in 1980–2012. Solid and dotted lines represent lines in 1950–1979 and 1980–2012, respectively. Blue and red points represent data of 1950–1979 and 1980–2012, respectively.

This downward movement denote the capacity of runoff yield decline. For the HURB (Figure 6b) and LRB (Figure 6d), the fitting lines moved upward, which illustrates that the capacity of runoff yield was enhanced. In the southern rivers, the runoff capacity of the PRB declined after 1980 (Figure 6g), whereas the change of MRB was not obvious (Figure 6f). The YARB also remained stable (Figure 6h). The streamflows of the TRB and HIRB in the northwest and the LCRB and YZRB in the southwest, originating from Tibet–Qinghai Plateau, were recharged by rainfall in addition to runoff from glacier and snow melt water. In this condition, the rainfall-runoff fitting lines could not fully reflect the changes in runoff yield ability. Nevertheless, the fitting lines can still be used to determine the role of rainfall change on runoff. The slope of the regression line in the HIRB during 1950–1979 was a negative value (Figure 6i), which shows that the water supply in addition to rainfall decreased. In 1980–2010, however, this part of the water supply increased. Similarly, the runoff yield in the TRB (Figure 6j) and the YZRB (Figure 6k) decreased, whereas the change in the LCRB was not obvious (Figure 6l). Changes in the rainfall–runoff relationship showed that the underlying surface affected the hydrological process, which will be further discussed in subsequent sections.

4.2. Monsoons

To determine the possible causes of streamflow variation, we examined Asian monsoon indices, including the East Asian monsoon index (EAMI), South Asian monsoon index (SAMI), Tibet–Qinghai Plateau monsoon index (TPMI), West Pacific subtropical high (WPSH), and westerly index (WI). The Asian monsoon indices were created by Li [46,47], and WI was derived from National Centers for Environmental Prediction (NCEP) reanalysis data. The TPMI was calculated from NCEP 600 mb height reanalysis data based on the method given by Wang [48].

Figure 7 shows the cumulative anomaly curves of runoff *versus* climatic indexes and their correlation coefficients. The streamflow in the northern rivers correlated positively with the EAMI and negatively with the WI, including the HRB (Figure 7a,b), HURB (Figure 7c,d), YRB (Figure 7e,f), LRB (Figure 7g,h), and SRB (Figure 7i,j). Among the northern rivers, the correlation coefficient between the YRB and EAMI streamflow was the highest ($R = 0.82$, $P < 0.001$). However, the cumulative anomaly curves of streamflow against the WI presented an opposite phase ($R = -0.83$, $P < 0.001$). The results showed that streamflow in the YRB was jointly affected by the East Asian monsoon and westerlies, which also reflects the interaction of westerlies and the East Asian monsoon. The relationship of streamflow in the HRB, HURB, LRB, and SRB and climatic indices was essentially the same as that in the YRB. However, the correlation was not as strong as that with the YRB, which may be related to the locations of the East Asia monsoon and westerly belt, as well as the influence of human activities on natural runoff. In the southeastern rivers, the runoff of the MRB was affected mainly by the West Pacific subtropical high ($R = 0.46$, $P < 0.01$) and the Tibet–Qinghai Plateau Monsoon ($R = 0.38$, $P < 0.01$) (Figure 7k,l). The PRB (Figure 7m,n) is adjacent to the South China Sea and is also located in the westerly belt and the East Asian monsoon zone. Therefore, its runoff was influenced by several monsoon systems and therefore lacked direct correlation with a specific monsoon index; the closest relationships were with the SAMI ($R = 0.24$, $P < 0.1$) and TPMI ($R = -0.55$, $P < 0.01$). The case of the YARB (Figure 7o,p) was similar to that of the PRB. The runoff was influenced by several monsoon systems dominated by the WI ($R = 0.64$, $P < 0.001$) and TPMI ($R = 0.39$, $P < 0.01$). Ma [49] also found a similar

phenomenon, although deeper indications require further investigation. In northwestern China, runoff in the HIRB (Figure 7q,r) and TRB (Figure 7s,t) correlated positively with that in the TPMI and WI, indicating that streamflow changes in these areas were controlled mainly by the Tibet–Qinghai Plateau monsoon and westerlies.

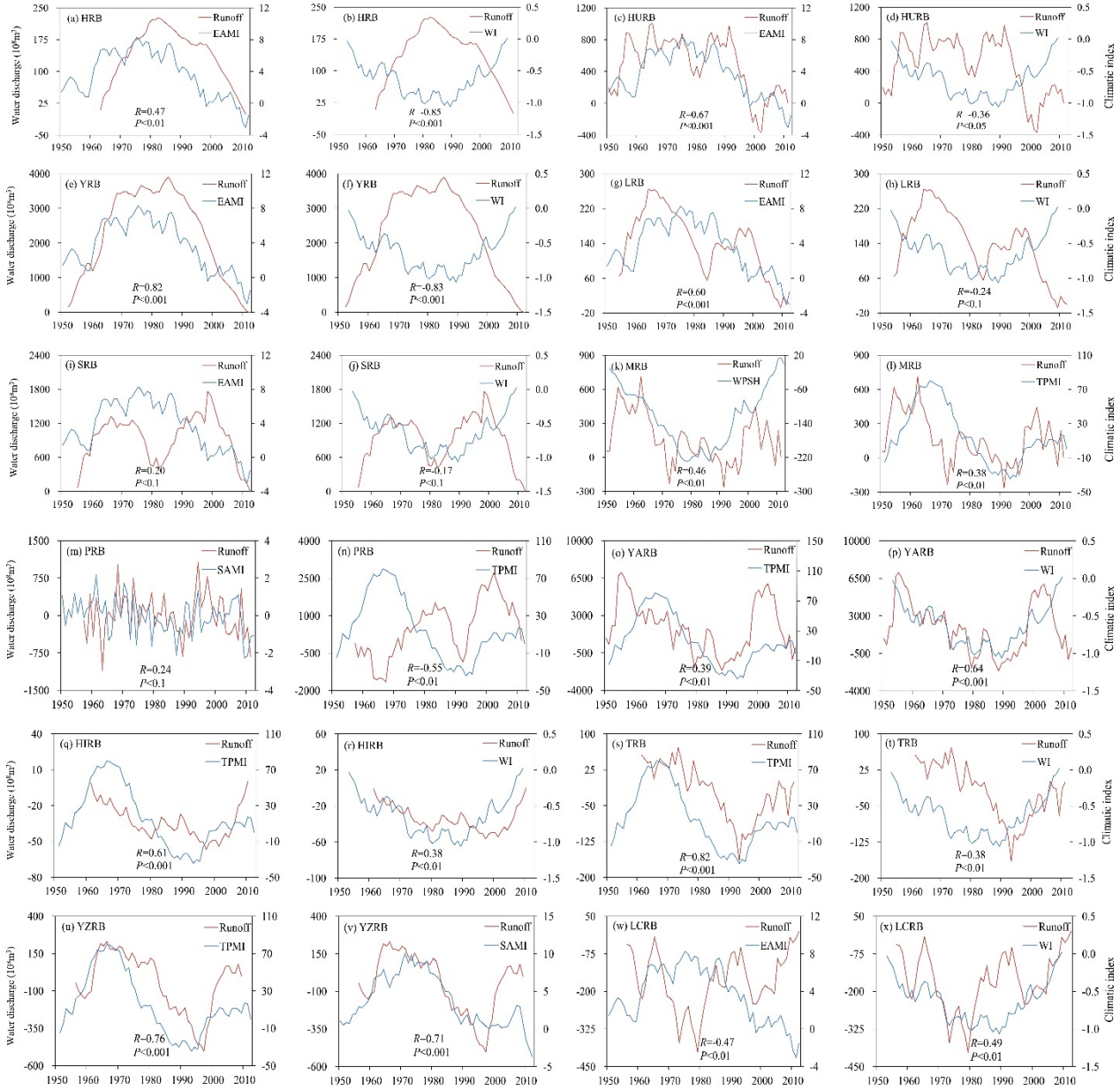

Figure 7. Cumulative anomaly curves of streamflow *versus* monsoon intensity indices in the main basins of China. EAMI, SAMI, WI, WPSH and TPMI represent the East Asian monsoon index, westerly index, West Pacific subtropical high, and Tibetan Plateau monsoon index, respectively. *R* and *P* represent the correlation coefficient and significance level, respectively.

A deeper indication is that the TRB and HIRB were located in the central area of Eurasia, which could have hardly been reached by the Northwest Pacific summer monsoon. Therefore, the westerlies and Tibet–Qinghai Plateau monsoon became the dominant factors. In southwestern China, the YZRB

originated from the Tibet–Qinghai Plateau hinterland. Its runoff was therefore subjected to the Tibet–Qinghai plateau monsoon, and the correlation coefficient between them was as high as 0.76 ($p < 0.001$) (Figure 7u,v). In contrast, because the YZRB was near the India Ocean, the runoff and particularly the midstream was influenced by the South Asia monsoon. In the LCRB (Figure 7w,x), although its headwater was in the Tibet–Qinghai Plateau monsoon zone, the runoff was mainly affected by the westerlies and East Asian monsoon.

4.3. Water Consumption for Industrial and Residential Purposes

Although climate change is important, particularly the impact of precipitation change on runoff, water consumption for industrial and residential purposes also plays important roles in runoff change [50–52]. Long-term statistics of water consumption are not currently available, which makes detailed analysis difficult. The "China Water Resources Bulletin (2004–2012)", reported that the YARB had the largest annual water consumption (Figure 8a). Aside from a slight reduction in water consumption in the HRB, the other basins all presented increasing trends in 2004–2012 (Figure 8a). Water for agriculture and industry accounted for the largest proportion at more than 80% of the total water consumption (Figure 8b,c). For long term trends, the "China Statistical Yearbook (1950–2009)" reported that the population, gross domestic product (GDP), and gross agricultural products showed significantly increasing trends (Figure 9). In particular, definite increases in water consumption are expected by the former two sectors. Thus, it can be inferred that the water consumption during the past 60 years also showed sharp increasing trends.

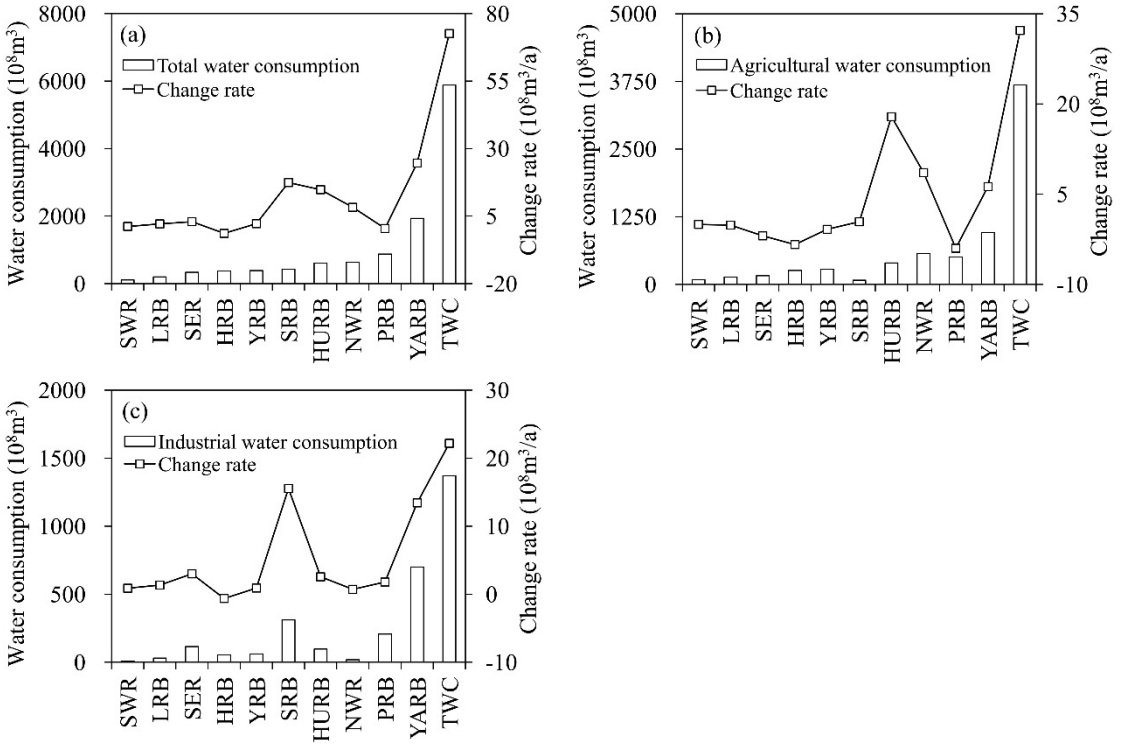

Figure 8. Interannual variability of water consumption and its change rate in the 10 major basins and in the whole country (TWC). (**a**), (**b**), and (**c**) are respectively gross water consumption, agricultural water consumption, and industrial water consumption.

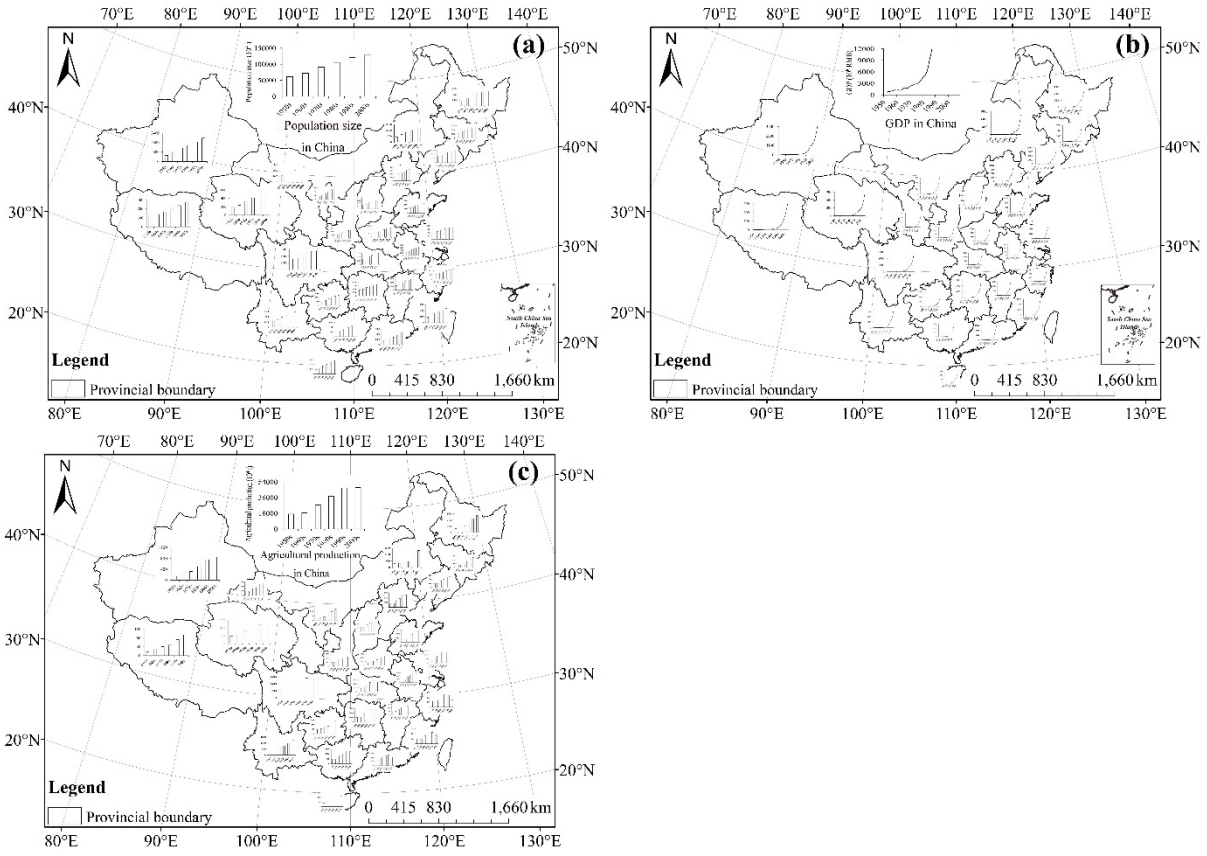

Figure 9. (**a**) Interannual variability of population; (**b**) gross domestic product (GDP); and (**c**) agricultural products in 1950–2012 in China.

4.4. Land Use/Land Coverage Change

The statistics of land use change from 1985 to 2010 are listed in Table 5. National land use change during the past 30 years shows obvious spatial differences and can be divided into two periods: from the end of the 1980s to 2000 and from 2000 to 2010. The characteristics of land use change during the first period indicate that farmland, residential land, industrial land, paddy fields, and water areas increased rapidly, and ecological land was greatly reduced. In 2000–2010, growth in farmland, residential land, paddy fields, and water areas slowed, and ecological land decreased slightly. Three possible causes can be considered. Firstly, construction land expansion was the main cause of the farmland decrease in traditional agricultural areas. In addition, large-scale ecological engineering promoted decreases in farmland. Another aspect, annual accumulated temperature increases in the northern arid zone, created suitable climatic conditions for reclamation in some forest zones, and a large area of dry land was converted to paddy fields. Secondly, implementation of the Reform and Opening-up policy resulted in rapid urbanization processes that occupied farmland and ecological land, particularly in eastern China. Thirdly, before 2000, the reclamation of grassland and forests caused soil degradation, which induced severe soil erosion. After 2000, the 'Grain for Green' program was implemented, which significantly increased the areas of grassland and forests in the ecologically fragile areas of western China.

Table 5. Area of land use conversion in China during the two periods of 1980s–2000 and 2000–2010.

Transfer Types	Dryland–Paddy Field	Grassland–Forest	Others–Waters	Others–ConstructionLand	Forest–Farmland	Forest–Grassland	Grassland–Farmland	Grassland–Forest	Waters–Others
1980–2000	173.15	115.80	80.81	177.63	174.73	81.14	345.76	104.73	62.40
2000–2010	138.12	142.36	114.55	378.24	37.54	41.85	197.38	88.79	83.27

The potential hydrological effect of land use/land coverage change has been a highly contested issue. Firstly, the high intensity of human activities in the city have resulted in accelerated soil compaction and crusting processes, thereby decreasing the infiltration rate and capacity of soil water storage and resulting in surface runoff increases [22,53]. Secondly, the runoff coefficients of forest areas and grassland are relatively small. When the forests and grassland converted to arable land, the flow yield will therefore increase. Thirdly, in southern China, a certain degree of lake reclamation occurred, which inhibited the process of evaporation and infiltration and resulted in runoff increases.

5. Influencing Factors of Sediment Load Variation

5.1. Hydraulic Engineering and Soil and Water Conservation Engineering

5.1.1. Soil and Water Conservation Engineering

China began to conduct soil and water conservation projects in the early 1950s, which included the construction of silt dams and terraced fields and the planting of trees and grass [54,55]. In the middle reaches of the Yellow River, for example, the most severe soil erosion in China occurred. The statistics of soil and water conservation engineering projects conducted in this area in 1979, 1989, 1996, and 2011 are plotted in Figure 10a.

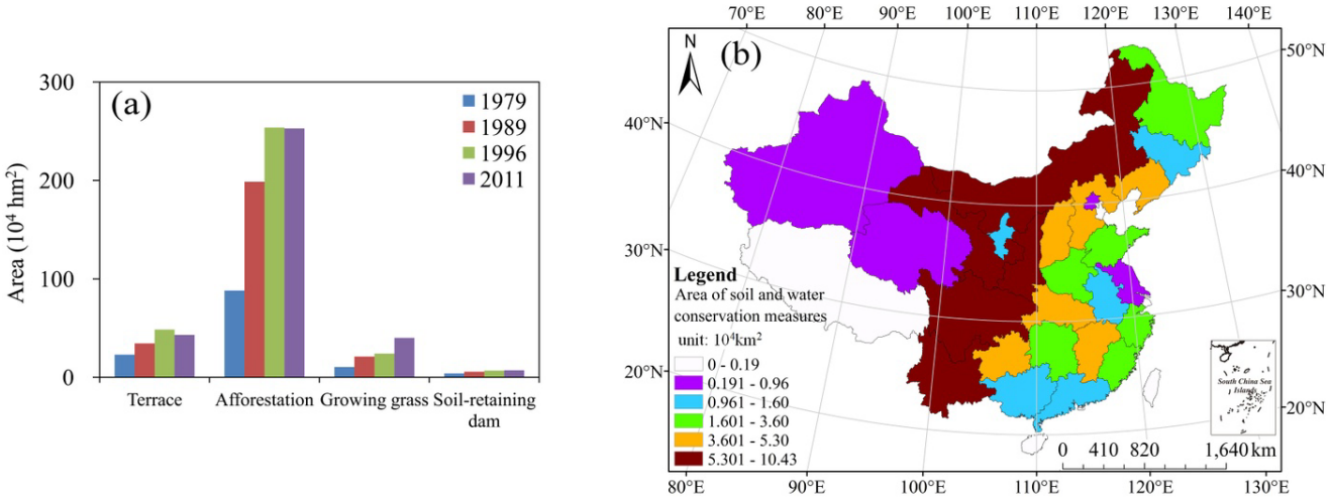

Figure 10. Statistics of soil and water conservation engineering areas in (**a**) the middle stream of the Yellow River basin (YRB) and (**b**) the national distribution.

All types of engineering showed an increasing trend, with the largest area in afforestation. On the national scale, the total area of present soil and water conservation engineering projects is 99.2 × 10^4

km^2, and the area of silt dams is 925.6 km^2 [56]. The largest distribution is in western China, which incurred severe soil erosion (Figure 10b). During the past 60 years, the runoff in some large rivers declined significantly (Figure 3), largely due to the impact of soil and water conservation engineering.

5.1.2. Reservoir and Dam Construction

By the end of 2012, the total number of large, medium, and small reservoirs in mainstreams and tributaries was 97,543, and a capacity of 8255×10^8 m^3 [56]. These reservoirs regulated the runoff and sediment change processes and reduced the sediment load in the downstream regions. The statistics of the "Water Resources Yearbook in 2006" [57] indicate that by the end of 2006, the numbers of large and medium reservoirs in the YARB were 149 and 1115, respectively, which ranked as highest. For the southern rivers including the YARB, PRB, HURB, and SERB, water resources were abundant. Thus, there were many reservoirs in these basins, and the ratios of total reservoir capacity (TRC) to average annual flow (AAF) was below 70%. However, in the northern rivers including the LRB, SRB, and HRB, the water resources are relatively limited; thus, the TRC/AAF was above 100%. In the two largest basins (YRB and YARB), the total amount of sedimentation in all of the reservoirs in the YARB during 1991–2005 was 17958×10^4 t. For the Sanmenxia and Xiaolangdi reservoirs, sedimentation in 1960–2012 and 1997–2012 was 64.108×10^8 m^3 and 27.625×10^8 m^3, respectively [56].

5.1.3. Water and Sediment Diversion Projects

To resolve the uneven distribution of water resources and to ease the high demand of local water resources, China has been conducting water and sediment diversion projects such as the "South-to-North Water Diversion Project" and the "Yellow River-to-Tianjin Water Diversion Project". After implementation of these projects, the streamflow and sediment load decreased in water supply areas and increased in water demand areas. In the "South-to-North Water Diversion Project", the amount of water diversion from the midstream region of the Yangtze River accounted for a very small proportion of the average streamflow, particularly in the wet seasons, and had little impact in abundant water. In the dry seasons, however, the water diversion project reduced the streamflow in the downstream region. Therefore, the saltwater traced back into the estuary of Yangtze River, and the sediment load was reduced downstream.

In the Yellow River, for example, the total amount of water diversion in the lower reaches was 3665.2×10^8 m^3 in 1958–2002, and the annual water diversion was 89.4×10^8 m^3, accounting for 23.1% of the runoff observed at Huayuankou Station during the same period and directly influencing streamflow and sediment changes in the lower reaches [23,55]. The amount of water and sediment diversion in the downstream region of the Yellow River in 2011 is shown in Table 6. These factors accounted for 15.6% and 13.6% of water and sediment discharge, respectively, during the same period.

Table 6. Amount of water and sediment diversion in the downstream reaches of the Yellow River in 2011.

Channel Segment	Xixiayuan–Huayuankou	Huayuankou–Jiahetan	Jiahetan–Gaocun	Gaocun–Sunkou	Sunkou–Aishan	Aishan–luokou	Luokou–Lijin	Lower Reaches of Lijin	Total
Length (km)	109.8	100.8	77.1	118.2	63.9	101.8	167.8	110.0	849.4
Amount of water diversion (10^8 m^3)	4.19	14.57	17.31	11.50	8.5	21.07	22.08	4.66	103.88
Amount of sediment diversion (10^4 t)	62.8	111.3	286.6	242.7	266.3	800.2	464.4	94.5	2328.8

5.2. Other Human Activities

The impacts of human activities on soil and water loss and sediment discharge in rivers include direct and indirect effects. Direct impacts include the erosion-transport-accumulation process induced by human activities such as farmland reclamation, mining, and road construction. The indirect impacts were mainly caused by destruction of vegetation, which accelerated the occurrence and development of soil erosion. With the development of society and the economy, both the strength and breadth of human activities were greater than those in the past. These activities include increases in population, the scale of reclamation, mining, and other infrastructure construction.

6. Impacts of Water and Sediment Discharge Reduction on Utilization of Sediment Resources

6.1. Effects of River Regulation and Flood Control

In the YRB, the sediment load in the lower reaches of Yellow River was greatly reduced in recent decades. Particularly after 2000, the streamflow and sediment load observed at Huayuankou Station were reduced by 52.5% and 61.7%, respectively, compared with those observed in the 1950s to 1960s. Reducing water and sediment discharges has relieved flood pressure and has influenced river regulation to some degree. Dike reinforcement with silt remains a very important project in the lower reaches of the Yellow River [58]. Decreases in sediment concentration by flooding and the threat of beach inundation by flooding have resulted in significant increases in the cost of dike reinforcement with silt.

6.2. Effects of Flood Irrigation and Soil Improvement

The sediment of the Yellow River, particularly flood sediment, is an effective material for soil improvement because it reduces salinity and alkalinity and improves land fertility. Until the early 1990s, the area of soil improvement was 23.2×10^4 hm^2 in the lower reaches of the Yellow River [58]. Soil improvement by silt is usually conducted during the flood season, when the sediment concentration is relatively high. However, this effect will be limited under the reduction of water and sediment resources.

6.3. Effects of Land and Wetland Formation

In the estuary area of the Yellow River, approximately 64% of sediment is precipitated on land and in shallow water, which elevates the riverbed and delta. The Linjin Station observation reported reductions of 88.7% and 67.5% in sediment and water discharge, respectively, compared with values reported in the 1950s and 1960s. Therefore, the land formation rate has decreased. For example, the 23.6 km^2/a land formation rate in 1855–1954 decreased to 8.6 km^2/a in 1992–2001 [58]. In addition, soil, water, and sediment are the main components of wetlands. Therefore, sediment and water discharge reduction will directly affect the quality and formation rate of wetlands.

7. Conclusions

The results of the present study are summarized in the following points:

1. During the past 60 years, the streamflow in northern China, including the HRB, HURB, YRB, LRB, and SRB, showed different decreasing trends. That in the southern rivers, including MRB, PRB and YARB, presented severe fluctuations, although the declining trend did not reach significant levels. For the streamflow in the TRB, HIRB, YZRB, and LCRB, increasing trends were presented. The runoff yield capacity was weakened in the HRB, YRB, SRB, and PRB and enhanced in the LRB and HURB. That in the MRB and YARB remained stable.
2. In the northern rivers, runoff correlated positively with the EAMI and negatively with the WI. In the southern rivers, runoff was mainly influenced by the Tibet–Qinghai monsoon, South Asian monsoon, and westerlies. That in the HIRB and TRB was controlled mainly by the Tibet–Qinghai monsoon and westerlies. Runoff in the YZRB was controlled by the South Asian monsoon and the Tibet–Qinghai monsoon, whereas that in the LCRB was influenced mainly by the East Asian monsoon and westerlies.
3. Sediment loads in the LCRB and YZRB did not present significant change trends. However, sediment loads in other rivers exhibited varying degrees of gradual reduction, the greatest of which was in the 2000s.
4. Underlying surface and precipitation changes jointly influenced the runoff in eastern rivers. Water consumption for industrial and residential purposes, soil and water conservation engineering projects, hydraulic engineering, and underlying surface changes induced by other factors were the main causes of runoff and sediment reduction.

Acknowledgments

This research was jointly funded by a key consulting project from the Chinese Academy of Engineering (2014-XZ-31), the National Natural Science Foundation of China (41301632) and the Chinese Research Academy of Environmental Sciences special funding for basic scientific research (2014-YKY-003).

Author Contributions

Chong Jiang, Fen Li and Linbo Zhang conceived the research idea and designed the methodology, Chong Jiang and Fen Li performed the analyses, and Chong Jiang, Daiqing Li, Fen Li, and Linbo Zhang wrote the paper.

Conflicts of Interest

The authors declare no conflict of interest.

References

1. Alan, D.Z.; Justin, S.; Edwin, P.M.; Bart, N.; Eric, F.W.; Dennis, P.L. Detection of intensification in global and continental scale hydrological cycles: Temporal scale of evaluation. *J. Clim.* **2003**, *16*, 535–547.
2. Easterling, D.R.; Meehl, G.A.; Parmesan, C.; Changnon, S.A.; Karl, T.R.; Mearns, L.O. Climate extremes: Observations, modeling, and impacts. *Science* **2000**, *289*, 2068–2074.
3. Qiu, J. China drought highlights future climate threats. *Nature* **2010**, *465*, 142–143.
4. Zhang, J.Y.; He, R.M.; Qi, J.; Liu, C.S.; Wang, G.Q.; Jin, J.L.; A new perspective on water issues in north China. *Adv. Water Sci.* **2013**, *24*, 303–310.
5. Zhang, Y.J.; Hu, C.H.; Wang, Y.G. Analysis on variation characteristics and influential factors of runoff and sediment of Liaohe River Basin. *Yangtze River* **2014**, *45*, 32–35.
6. World Water Assessment Programme (WWAP). *The United Nations World Water Development Report 4: Managing Water under Uncertainty and Risk*; World Water Assessment Programme: Paris, France, 2012.
7. Vörösmarty, C.J.; McIntyre, P.B.; Gessner, M.O.; Dudgeon, D.; Prusevich, A.; Green, P.; Glidden, S.; Bunn, S.E.; Sullivan, C.A.; Liermann, C.R.; *et al*. Global threats to human water security and river biodiversity. *Nature* **2010**, *467*, 555–561.
8. Intergovernmental Panel on Climate Change (IPCC). *Managing the Risks of Extreme Events and Disasters to Advance Climate Change Adaptation*; Cambridge University Press: Cambridge, UK, 2012.
9. Climate Change 2013: The Physical Science Basis, Summary for Policy Makers, Technical Summary and Frequently Asked Questions. Available online: https://www.ipcc.ch/pdf/assessment-report/ar5/wg1/WG1AR5_SummaryVolume_FINAL.pdf (accessed on 13 October 2015).
10. Matthew, B.C.; Nigel, W.A. Adapting to climate change impacts on water resources in England-An assessment of draft water resources management plans. *Glob. Environ. Chang.* **2011**, *21*, 238–248.
11. Domroes, M.; Peng, G. *The Climate of China*; Springer: Berlin, Germany, 1988.
12. Zhai, P.M.; Zhang, X.B.; Wan, H.; Pan, X.H. Trends in total precipitation and frequency of daily precipitation extremes over China. *J. Clim.* **2005**, *18*, 1096–1108.
13. Ding, Y.; *Monsoons Over China*; Kluwer Academic Publishers: Amsterdam, the Netherland, 1994.
14. Holeman, J.N. The sediment yield of major rivers of the world. *Water Resour. Res.* **1968**, *4*, 737–747.

15. Holland, H.D. River transport to the oceans. In *The Ocean Lithosphere*; John Wiley & Sons: New York, NY, USA, 1981.
16. Walling, D.E.; Fang, D. Recent trends in the suspended sediment loads of the world rivers. *Glob. Planet. Chang.* **2003**, *39*, 111–126.
17. Milliman, J.D. Delivery and fate of fluvial water and sediment to the sea: A marine geologist's view of European rivers. *Sci. Mar.* **2001**, *65*, 121–132.
18. Bobrovitskaya, N.N.; Kokorev, A.V.; Lemeshko, N.A. Regional patterns in recent trends in sediment yields of Eurasian and Siberian rivers. *Glob. Planet. Chang.* **2003**, *39*, 127–146.
19. Liu, C.; Wang, Y.G.; Sui, J.Y. Analysis on variation of seagoing water and sediment load in main rivers of China. *J. Hydraul. Eng.* **2007**, *38*, 1444–1452.
20. Subramainian, V. Sediment load of Indian rivers. *Curr. Sci.* **1993**, *64*, 928–930.
21. Siakeu, J.; Oguchi, T.; Aoki, T.; Esakid, Y.; Jarviee, H.P. Change in riverine suspended sediment concentration in central Japan in response to late 20th century human activities. *Catena* **2004**, *55*, 231–254.
22. Wang, Y.G.; Liu, X.; Shi, H.L. Variation and influence factor of runoff and sediment in the lower and middle Yangtze River. *J. Sed. Res.* **2014**, *29*, 38–47.
23. Miao, C.Y.; Ni, J.R.; Borthwick, A.G.L. Recent changes of water discharge and sediment load in the Yellow River basin. *Prog. Phys. Geogr.* **2010**, *34*, 541–561.
24. Shi, H.L.; Hu, C.H.; Wang, Y.G.; Tian, Q.Q. Variation trend and cause of runoff and sediment load variations in Huaihe River. *J. Hydraul. Eng.* **2012**, *43*, 571–579.
25. Zhang, J.Y.; Zhang, S.L.; Wang, J.X.; Li, Y. Study on runoff trends of the six larger basins in China over the past 50 years. *Adv. Water Sci.* **2007**, *18*, 230–234.
26. Miao, C.Y.; Yang, L.; Liu, B.Y.; Gao, Y.; Li, S.L. Streamflow changes and its influencing factors in the mainstream of the Songhua River basin, Northeast China over the past 50 years. *Environ. Earth Sci.* **2011**, *63*, 489–499.
27. Yang, S.L.; Zhao, Q.Y.; Belkin, I.M. Temporal variation in the sediment load of the Yangtze River and the influences of the human activities. *J. Hydrol.* **2002**, *263*, 56–71.
28. Gao, G.; Chen, D.L.; Xu, C.Y.; Simelton, E. Trend of estimated actual evapotranspiration over China during 1960–2002. *J. Geophys. Res.* **2007**, *112*, D11120.
29. International Research and Training Center on Erosion and Sedimentation (IRTCES) China. *Gazette of River Sedimentation 2011*; China Water Power Press: Beijing, China, 2012.
30. Lu, X.X.; Higgitt, D.L.; Sediment yield variability in the upper Yangtze, China. *Earth Surf. Proc. Land* **1999**, *24*, 1077–1093.
31. Hassan, M.A.; Church, M.C.; Xu, J.X.; Yan, Y.X. Spatial and temporal variation of sediment yield in the landscape: Example of Huanghe (Yellow River). *Geophys. Res. Lett.* **2008**, *35*, L06401.
32. Mann, H.B. Non-parametric tests against trend. *Econometrica* **1945**, *13*, 245–259.
33. Kendall, M.G. *Rank Correlation Methods*; Griffin: London, UK, 1975; pp. 1–200.
34. Chattopadhyay, S.; Jhajharia, D.; Chattopadhyay, G. Trend estimation and univariate forecast of the sunspot numbers: Development and comparison of ARMA, ARIMA and Autoregressive Neural Network models. *C.R. Geosci.* **2011**, *343*, 433–442.
35. Theil, H. A rank invariant method of linear and polynomial regression analysis. *Proc. R. Neth. Acad. Sci.* **1950**, *53*, 1397–1412.

36. Sen, P.K. Estimates of the regression coefficients based on Kendall's tau. *J. Am. Stat. Assoc.* **1968**, *63*, 1379–1389.
37. Jhajharia, D.; Dinpashoh, Y.; Kahya, E.; Choudhary, R.R.; Singh, V.P. Trends in temperature over Godavari River basin in Southern Peninsular India. *Int. J. Climatol.* **2013**, *34*, 1369–1384.
38. Misuses of statistical analysis in climate researchvon; In *Analysis of Climate Variability: Applications of Statistical Techniques*; Storch, H., Navarra, A., Eds.; Springer: Berlin, Germany, 1995; pp. 11–26.
39. Chattopadhyay, S.; Jhajharia, D.; Chattopadhyay, G. Univariate modeling of monthly maximum temperature time series over northeast India: Neural network *versus* Yule-walker equation based approach. *Meteorol. Appl.* **2011**, *18*, 70–82.
40. Kumar, S.; Merwade, V.; Kam, J.; Thurner, K. Streamflow trends in Indiana: Effects of long term persistence, precipitation and subsurface drains. *J. Hydrol.* **2009**, *374*, 171–183.
41. Xu, J.X. Recent variations in water and sediment in relation with reservoir construction in the upper Changjiang River Basin. *J. Mount. Sci.* **2009**, *27*, 385–393.
42. Merriam, C.F. A comprehensive study of the rainfall on the susquehanna valley. *Trans. Amer. Geophys. Union* **1937**, *18*, 471–476.
43. Searcy, J.K.; Hardisoni, C.H.; Langbein, W.B. *Double Mass Curves*; Geological Survey Water Supply Paper 1541-B; US Geological Survey: Washington, DC, USA, 1960.
44. Mu, X.M.; Zhang, X.Q.; Gao, P.; Wang, F. Theory of double curves and its applications in hydrology and meteorology. *J. China Hydrol.* **2010**, *30*, 47–51.
45. Li, Y.Y.; Cao, J.T.; Shen, F.X.; Xia, J. The changes of renewable water resources in China during 1956–2010. *Sci. China Earth Sci.* **2014**, *57*, 1825–1833.
46. Li, J.P.; Wu, Z.W.; Jiang, Z.H.; He, J.H. Can global warming strengthen the East Asian summer monsoon? *J. Clim.* **2010**, *23*, 6696–6705.
47. Li, J.P.; Feng, J.; Li, Y. A possible cause of decreasing summer rainfall in northeast Australia. *Int. J. Climatol.* **2011**, *31*, doi:10.1002/joc.2328.
48. Wang, M.C.; Liang, J.; Shao, M.J.; Shi, G. Preliminary analysis on interannual change of Tibet–Qinghai Plateau monsoon. *Plateau Meteorol.* **1984**, *3*, 76–82.
49. Ma, H.; Yang, D.W.; Tan, S.K.; Gao, B.; Hu, Q.F. Impact of climate variability and human activity on streamflow decrease in the Miyun Reservoir catchment. *J. Hydrol.* **2010**, *389*, 317–324.
50. Chen, Y.N.; Fan, Y.T.; Wang, H.J.; Fang, G.H. Research progress on the impact of climate change on water resources in the arid region of Northwest China. *Acta Geogr. Sin.* **2014**, *69*, 1295–1304.
51. Song, X.M.; Zhang, J.Y.; Zhan, C.S.; Liu, C.Z. Review for impacts of climate change and human activities on water cycle. *J. Hydraul. Eng.* **2013**, *44*, 779–790.
52. He, D.M.; Liu, C.M.; Feng, Y.; Hu, J.M.; Ji, X.; Li, Y.G. Progress and perspective of international river researches in China. *Acta Geogr. Sin.* **2014**, *69*, 1284–1294.
53. Liu, C.; Hu, C.H.; Shi, H.L. Changes of runoff and sediment fluxes of river in mainland of China discharge into Pacific Ocean. *J. Sed. Res.* **2012**, *27*, 70–75.
54. Liu, C.; He, Y.; Zhang, H.Y. Trends analysis of the water and sediment loads of the main rivers in China using water-sediment diagram. *Adv. Water Sci.* **2008**, *19*, 317–324.

55. Liu, C.; Wang, Z.Y.; Sui, J.Y. Variation of flow and sediment of the Yellow River and their influential factors. *Adv. Sci. Technol. Water Resour.* **2008**, *28*, 1–7.
56. Ministry of Water Resources of the People's Republic of China (MWRPRC). *Chinese River Sediment Bulletin 2012*; China Water Power Press: Beijing, China, 2013; pp. 1–60.
57. Ministry of Water Resources of the People's Republic of China (MWRPRC). *Chinese River Sediment Bulletin 2006*; China Water Power Press: Beijing, China, 2007; pp. 1–55.
58. Wang, Y.G.; Hu, C.H.; Shi, H.L. Variation in water and sediment resources and its influence on utilization of sediment resource in the Yellow River Basin. *J. China Inst. Water Resour. Hydropower Res.* **2010**, *8*, 237–245.